SNI
SURGICAL NEUROLOGY INTERNATIONAL
SNI: Neurovascular
OPEN ACCESS
For entire Editorial Board visit : http://www.surgicalneurologyint.com
Editor: James I. Ausman, MD, PhD University of California, Los Angeles, CA, USA

Original Article

Smaller outer diameter of atherosclerotic middle cerebral artery associated with *RNF213* c.14576G>A Variant (rs112735431)

Hiroki Hongo, Satoru Miyawaki, Hideaki Imai, Yuki Shinya, Hideaki Ono, Harushi Mori[1], Hirofumi Nakatomi, Akira Kunimatsu[1], Nobuhito Saito

Departments of Neurosurgery and [1]Radiology, Faculty of Medicine, The University of Tokyo, Tokyo, Japan

E-mail: Hiroki Hongo - hhongo@hotmail.co.jp; *Satoru Miyawaki - miyawaki-tky@umin.ac.jp; Hideaki Imai - hiimai-nsu@umin.ac.jp; Yuki Shinya - yukishinya6155@gmail.com; Hideaki Ono - hideono-tky@umin.ac.jp; Harushi Mori - hmori-tky@umin.ac.jp; Hirofumi Nakatomi - hnakatomi-tky@umin.ac.jp; Akira Kunimatsu - KUNIMATSUA-RAD@h.u-tokyo.ac.jp; Nobuhito Saito - nsaito-tky@umin.net
*Corresponding author

Received: 08 February 17 Accepted: 20 March 17 Published: 05 June 17

Abstract

Background: Intracranial atherosclerosis (ICAS) involves diverse histologies and several remodeling patterns. Ring finger protein 213 (RNF213) c.14576G>A variant (rs112735431), recently reported to be associated with ICAS, may be linked with negative remodeling (outer diameter – reducing morphological alteration) of intracranial arteries. This study investigated the outer diameter of atherosclerotic middle cerebral artery (MCA).

Methods: Patients with unilateral atherosclerotic MCA stenosis/occlusion were enrolled in this single-hospital-based case-control study at The University of Tokyo Hospital. The patients were divided into two groups by the presence of RNF213 c.14576G>A (variant group and wild-type group) and the outer diameter of the MCA was measured with high-resolution magnetic resonance imaging.

Results: Twenty-eight patients with the wild type and 19 patients with the variant type were included. The outer diameter of the stenotic side MCA was smaller in the variant group than in the wild-type group ($P = 8.3 \times 10^{-6}$). The outer diameter of the normal side MCA was also smaller in the variant group than in the wild-type group ($P = 5.2 \times 10^{-3}$). The ratio of stenotic side to normal side was also smaller in the variant group than in the wild-type group ($P = 1.5 \times 10^{-5}$).

Conclusions: This study indicates that RNF213 c.14576G>A is associated with negative remodeling of ICAS.

Key Words: Atherosclerosis, remodeling, genetics, intracranial artery stenosis, magnetic resonance imaging (MRI), RNF213

Access this article online
Website: www.surgicalneurologyint.com
DOI: 10.4103/sni.sni_59_17
Quick Response Code:

INTRODUCTION

Intracranial atherosclerosis (ICAS) is one of the main causes of ischemic stroke.[36] The degree of intracranial artery stenosis is an important predictor of ischemic stroke in patients with ICAS, so evaluation of ICAS has mainly been based on assessment of the intraluminal status of atherosclerotic arteries.[17] However, the morphological

How to cite this article: Hongo H, Miyawaki S, Imai H, Shinya Y, Ono H, Mori H, *et al*. Smaller outer diameter of atherosclerotic middle cerebral artery associated with *RNF213* c.14576G>A Variant (rs112735431). Surg Neurol Int 2017;8:104.
http://surgicalneurologyint.com/Smaller-outer-diameter-of-atherosclerotic-middle-cerebral-artery-associated-with-*RNF213*-c.14576G>A-Variant-(rs112735431)/

characteristics of the arterial wall of the stenotic lesion of ICAS have recently received much attention.[44]

Classification of arterial remodeling patterns is one of the widely used evaluation methods for arterial wall morphological characteristics. Progress in imaging technology such as high-resolution magnetic resonance imaging (MRI) has enabled the visualization of arterial morphological changes in ICAS,[12,43] and as reported in the coronary and other systemic arteries,[3,4,7,18,20,31,32,38,39] cerebral atherosclerotic lesions are known to exhibit considerable heterogeneity in morphological structures. Several arterial remodeling patterns, such as the "positive/negative" remodeling pattern, which is defined by the presence of outward expansion of the outer diameter, and the "eccentric/concentric" remodeling pattern, which is defined by the eccentricity of the wall morphology, have been reported previously.[1,8,28,30,40,41,43-45] As evaluation methods of wall morphology have advanced, differences in wall characteristics have emerged in association with the progression of ischemic stroke.[5,41,44,46]

Recently, we identified a genetic variant that has a strong association with ICAS.[23,24] This genetic variant is a single-base variant (nonsynonymous variant), c.14576G>A (p.R4859K, rs112735431) variant in *ring finger protein 213* (*RNF213*; a gene located in chromosome 17q; based on the National Center for Biotechnology Information Reference sequence NP_065965.4). This *RNF213* c.14576G>A variant (rs112735431) is present in approximately 25% of patients with ICAS in the Japanese population.[23,24]

RNF213 c.14576G>A was originally identified as a susceptibility gene variant of moyamoya disease (MMD), which is characterized by the progressive stenosis of the terminal portions of the bilateral internal carotid arteries.[2,14,21,22] Recently, negative remodeling has been reported to characterize the features of the arterial wall in MMD patients, which is defined as outer diameter-reducing morphological alteration of the arteries occurring with the progress of luminal stenosis.[13,19,29]

In the present study, we hypothesized that *RNF213* c.14576G>A, the genetic variant associated with ICAS, is also associated with negative remodeling of ICAS. To prove this hypothesis, we analyzed the outer diameter of the intracranial arteries of ICAS patients divided into two groups according to the presence of *RNF213* c.14576G>A.

MATERIALS AND METHODS

Patient population

This study prospectively enrolled patients with unilateral atherosclerotic middle cerebral artery (MCA) stenosis/occlusion who visited The University of Tokyo Hospital, Tokyo, Japan between April 2013 and December 2015. The criteria for inclusion were: (1) unilateral MCA (M1 portion) >50% stenosis/occlusion on magnetic resonance angiography (MRA); and (2) one or more risk factors of atherosclerosis including hypertension, diabetes mellitus, dyslipidemia, and history of cigarette smoking. Patients with non-atherosclerotic vasculopathy, such as dissection, vasculitis, or MMD, and evidence of cardioembolism were excluded. We also evaluated for the presence of symptoms. Symptomatic patients were defined as having both of MRI finding of cerebral ischemia in the distribution of the stenotic MCA and consistent focal neurological deficit.

MRI studies

MRI/MRA was performed in all patients. MRA was used to evaluate stenosis. Degree of luminal stenosis was classified into 5 intracranial artery stenosis (IAS) grades, according to a previously reported study, as: normal, no evidence of stenosis (grade 0); mild stenosis, <50% stenosis (grade 1); moderate stenosis, >50% stenosis (grade 2); severe stenosis, partial signal loss with the distal flow signal (grade 3); and occlusion, no distal flow signal (grade 4).[37] The outer diameter of M1 portion of MCA was measured at the greatest minor axis on axial fast imaging employing steady-state acquisition (FIESTA) MRI using a 3T-MRI scanner (Signa, HDxt 3T; GE Healthcare, Milwaukee, WI) and a 12-channel phased array head neck spine coil. Three-dimensional time-of-flight MRA was performed with the following parameters: repetition time (TR)/echo time (TE) = 26/2.9 ms, field of view (FOV) = 20 cm, thickness/intervals = 0.4/0.2 mm, matrix = 512 × 512, and number of excitations (NEX) = 1. Then, FIESTA MRI was obtained using the following parameters: TR/TE = 4.81/1.86 ms, FOV = 20 cm, slice thickness/intervals = 0.4/0.2 mm, matrix = 512 × 512, and NEX = 1. The voxel size was 0.4 × 0.4 × 0.2 mm^3 for both MRA and FIESTA.

Identification of RNF213 c.14576G>A variant (rs112735431)

Peripheral blood samples were obtained from all enrolled patients. Genomic DNA was obtained from the peripheral blood leukocytes at SRL, Inc. (Tachikawa, Tokyo, Japan) using a DNA extraction kit (Talent Srl, Trieste, Italy). Screening for the *RNF213* c.14576G>A was performed by direct Sanger sequencing in all cases. *RNF213* exon 61, which includes the c.14576G>A variant of *RNF213* (GenBank accession number, NM_020914.4), was amplified by polymerase chain reaction (PCR). The primers 5′-CTGCATCACAGGAAATGACACTG and 5′-TGACGAGAAGAGCTTTCAGACGA were used for amplification and sequencing, as reported previously.[21] PCR was performed in a total of 20 μL reaction mixture containing 50 ng of genomic DNA, 10 μL of 2× PCR

buffer, 4 μL of 2 mM deoxynucleotide triphosphate, 1 μL of each forward and reverse primers (20 μM), and 0.4 μL of 1 U/μL KOD FX Neo (TOYOBO Co., Ltd., Osaka, Japan). Initial denaturation was performed at 94°C for 2 minutes, followed by 35 cycles of amplification consisting of denaturation at 98°C for 10 s, annealing at 60°C for 30 s, and extension at 68°C for 30 s. The PCR products were treated with QIAquick Gel Extraction Kit (Qiagen N.V., Venlo, Netherlands) after agarose gel electrophoresis. Direct sequencing was performed at FASMAC Co., Ltd. (Atsugi, Kanagawa, Japan) using an ABI Genetic Analyzer 3130XL or ABI DNA Analyzer 3730xL (Applied Biosystems, Foster City, CA). Cycle sequencing was carried out using the BigDye Terminator v3.1 cycle sequencing kit (Applied Biosystems). Sequence chromatographs were analyzed with a Sequence Scanner version 1.0 (Applied Biosystems). All investigators involved in genotyping were unaware of the phenotypic information. All analyses of the sequenced data were performed at the Department of Neurosurgery, The University of Tokyo.

Statistical analysis

The Pearson Chi-square test was used to compare the clinical characteristics between the wild type group (patients with *RNF213* c.14576G>A wild type, GG) and variant group (patients with *RNF213* c.14576G>A variant both heterozygote and homozygote, AG and AA). The Mann–Whitney U test was used to compare non-normally distributed continuous variables, such as age and diameter of the intracranial arteries between the two groups. All analyses were performed using JMP Pro version 11.0.0 (SAS Institute, Inc., Cary, NC). *P* value less than 0.05 was considered to be statistically significant.

Ethical considerations

This study was approved by the Human Genome, Gene Analysis Research Ethics Committee of the Faculty of Medicine, The University of Tokyo (approval number: 3516; approval date: September 12, 2011). Written informed consents were obtained from all participants in this study.

RESULTS

Clinical characteristics

Table 1 shows the clinical characteristics of the patients including 28 patients with the wild type and 19 patients with the variant type. The distribution of IAS grade, mean age, number of women, and number of symptomatic patients were similar in the wild-type and variant groups. Patients with diabetes mellitus were significantly more common in the wild-type group than in the variant group ($P = 0.030$). The numbers of patients with hypertension, dyslipidemia, ischemic heart disease, arteriosclerosis obliterans, and history of cigarette smoking were not significantly different.

Outer diameter

Figure 1 represents examples of measurement of the outer diameter in both groups. Table 2 shows the

Table 1: Clinical characteristics of the study population

Characteristics	*RNF213* c. 14576G>A Genotype		*P*
	Wild Type (G/G)	Variant (A/G + A/A)	
Number of patients	28	19	
Genotype			
GG	28	0	
GA	0	18	
AA	0	1	
IAS grade, *n* (%)			
2	11 (39.3)	8 (42.1)	
3	5 (17.9)	5 (26.3)	
4	12 (42.8)	6 (31.6)	0.80
Age, mean±SD (range), y	62.1±12.9 (41-83)	61.2±11.3 (38-77)	0.64
Female, *n* (%)	12 (42.8)	11 (57.8)	0.31
Symptomatic, *n* (%)	7 (25.0)	4 (23.4)	0.75
Underlying diseases			
Hypertension	12 (42.8)	10 (52.6)	0.50
Diabetes	6 (21.4)	0 (0.0)	0.030
Dyslipidemia	5 (17.8)	6 (31.5)	0.27
Ischemic heart diseases	4 (14.2)	3 (15.7)	0.88
Arteriosclerosis obliterans	0 (0.0)	1 (5.2)	0.21
Smoking	6 (21.4)	6 (31.5)	0.43
Alcohol	5 (18.5)	5 (26.3)	0.48

IAS: Indicates intracranial artery stenosis, *RNF213*: *Ring finger protein 213*, SD: Standard deviation

Table 2: Results of measurement of outer diameter

	RNF213 c. 14576G>A Genotype		*P*
	Wild type (G/G) *n*=28	Variant (A/G + A/A) *n*=19	
Outer diameter on stenotic side, mm	2.94±0.57 (3.22, 1.7-3.8)	2.09±0.32 (2.17, 1.53-2.69)	8.3×10^{-6}
Outer diameter on normal side, mm	3.14±0.46 (3.24, 2.18-4.33)	2.80±0.33 (2.78, 2.17-3.27)	5.2×10^{-3}
Ratio	0.93±0.13 (0.94, 0.54-1.15)	0.75±0.11 (0.76, 0.51-0.93)	1.5×10^{-5}

Data are average±standard deviation (median, range). *RNF213*: Indicates *ring finger protein 213*

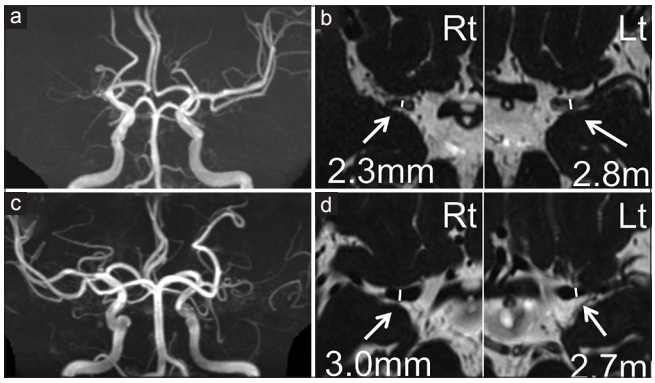

Figure 1: Representative cases are presented. MRA (a and c) and FIESTA images (b and d) of a 70-year-old man with RNF213 variant (a and b) and of a 72-year-old woman without RNF213 variant (c and d). Outer diameters of the bilateral M1 are shown. >50% stenosis or occlusion cases on MRA were included and the outer diameter of M1 was measured at the greatest minor axis in the proximal portion on axial FIESTA MRI. Rt indicates right side; Lt, left side

results of measurement. Figure 2 shows the box plots of the each value. In the wild-type group, the mean outer diameter was 2.94 ± 0.57 mm on the stenotic side and 3.14 ± 0.46 mm on the normal side. In the variant group, these values were 2.09 ± 0.32 mm and 2.80 ± 0.33 mm, respectively. The outer diameter of the stenotic side was smaller than the normal side in both groups. The outer diameter of the stenotic side was significantly smaller in the variant group than in the wild type group ($P = 8.3 \times 10^{-6}$). The outer diameter of the normal side was also significantly smaller in the variant group than in the wild-type group ($P = 5.2 \times 10^{-3}$). To investigate the influence of *RNF213* variant on remodeling, the ratio of the stenotic side to normal side was calculated and was found to be significantly smaller in the variant group (0.75 ± 0.11) than in the wild-type group (0.93 ± 0.13) ($P = 1.5 \times 10^{-5}$).

DISCUSSION

The present study found that the outer diameter of MCA atherosclerosis was smaller in patients with the *RNF213* c.14576G>A than in patients without the *RNF213* c.14576G>A. In addition, the ratio of the outer diameter of the stenotic side to the normal side in MCA atherosclerosis was smaller in patients with the *RNF213* c.14576G>A than in patients without *RNF213* c.14576G>A. These results indicate that *RNF213* c.14576G>A is associated with negative arterial remodeling in ICAS.

The histology of positive remodeling of atherosclerotic arteries in ICAS as well as other systemic arteries is known to involve lipid-rich plaque burden, intraplaque hemorrhage, fibrin cap, and infiltration of inflammatory cells.[5,7,9,12] However, the histological characteristics of negative remodeling is less well known, and few detailed histological findings have been reported. Negative remodeling of the coronary artery has been observed to involve shrinkage of the arterial wall resulting in stenotic lumen instead of intraluminal plaque deposition.[25-27,34] Assuming that negative remodeling ICAS undergoes similar histological changes, *RNF213* c.14576G>A might manifest as the morphological shrinkage of the arterial wall in ICAS. However, detailed histological findings of wall shrinkage in negative remodeling atherosclerosis have not been elucidated even in the coronary artery. To investigate the detailed effects of the *RNF213* c.14576G>A on ICAS, more histological observations of negative remodeling in ICAS are required.

The smaller outer diameter on the normal side in the variant group indicates that the *RNF213* c.14576G>A affects the outer diameter of normal intracranial arteries. Consequently, the present study identified *RNF213* c.14576G>A as a genetic factor in the structure of normal intracranial artery. This important result suggests that the *RNF213* c.14576G>A may affect either the morphogenesis or the morphological change of the intracranial artery. The present study investigated only ICAS patients classified by the presence of *RNF213* c.14576G>A, hence further study should compare the character-matched groups of healthy individuals classified by the presence of *RNF213* c.14576G>A to confirm the influence of *RNF213* c.14576G>A on the normal intracranial artery.

RNF213 encodes a protein with 5256 amino acids harboring a RING (really interesting new gene) finger motif and an AAA (adenosine triphosphatase associated with various cellular activities) domain, indicating the presence of both E3 ubiquitin ligase activity and energy-dependent unfoldase.[14,21] *RNF213* mRNA is ubiquitously expressed in various human tissues, but is especially highly expressed in immune tissues, such as

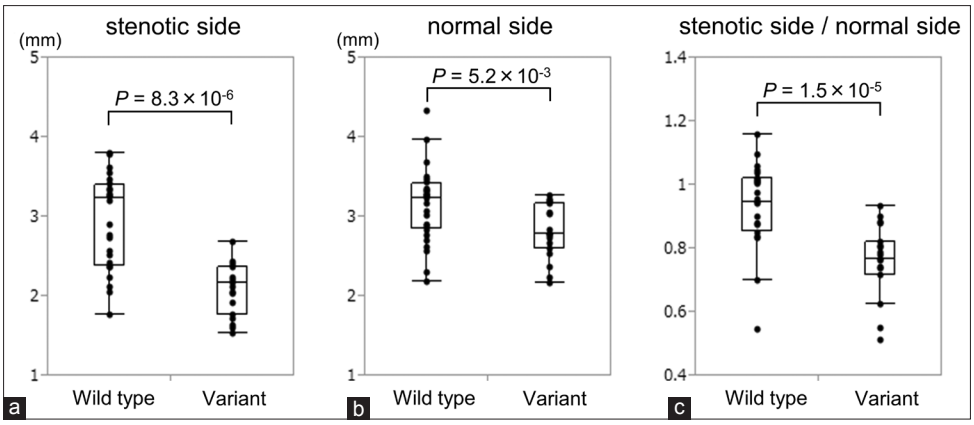

Figure 2: (a) A box plot of the outer diameters of M1 on the stenotic side of wild type and variant groups. Variant group had significantly smaller outer diameter on the involved side than the wild type group. (b) A box plot of the outer diameters of M1 on the normal side. The variant group also had significantly smaller outer diameter on the normal side than wild type group. (c) A box plot of the ratio of outer diameters of M1 on the stenotic side to the normal side. Variant group had significantly smaller ratio than the wild type group

the spleen and leukocytes.[14] Knockdown of *RNF213* in zebrafish caused irregular wall formation in trunk arteries and abnormal sprouting vessels, indicating the potential function of *RNF213* in the development of intracranial angiogenesis.[21] On the other hand, transgenically generated *RNF213*-deficient mice and *RNF213*-knock-in mice expressing a missense mutation in mouse *RNF213* p. R4828K on exon 61, corresponding to human *RNF213* p. R4859K, grow normally, with no significant differences in MRA findings or the anatomy of the circle of Willis compared with wild-type littermates.[15,35] These findings indicate that other secondary insults such as environmental factors besides *RNF213* deficiency are necessary for the onset of intracranial major artery stenosis and intracranial arterial remodeling. *In vitro* studies of induced pluripotent stem cell-derived vascular endothelial cells from patients with MMD and carriers of *RNF213* c.14576G>A variant showed lower angiogenic activities in the tube formation assay than in carriers of the wild-type variant, indicating the potential function of *RNF213* in endothelial cells.[10] Recently, the signaling pathways for the regulation of *RNF213*, such as interferon-beta signaling, and the relationship of *RNF213* with the known molecular pathways for vascular remodeling, such as non-canonical Wnt signaling, have gradually been identified.[16,33] However, the precise molecular mechanism by which the *RNF213* c.14576G>A causes human intracranial arterial remodeling is not completely understood, and further molecular biological functional analysis of *RNF213* is required.

Remodeling patterns are associated with the risk of ischemic stroke,[5,41,44,46] and so influence the therapeutic choice of ICAS. Conventionally, evaluation of the severity of luminal stenosis has mainly focused on the intracranial artery, and transluminal angioplasty has been considered as an effective therapeutic choice to improve ICAS and subsequent ischemic stroke.[11] The Stenting vs. Aggressive Medical Management for Preventing Recurrent Stroke in Intracranial Stenosis (SAMMPRIS) trial evaluated the effectiveness of intraluminal angioplasty, but failed to prove the efficacy of intracranial artery stenting, as the rate of periprocedural stroke after percutaneous transluminal angioplasty and stenting was higher than the estimated probability.[6] One important possible reason is that the SAMMPRIS trial included patients selected on the basis of angiographical arterial stenosis but the wall characteristics such as outer diameter and eccentricity were not evaluated. Therefore, patients with negative remodeling of stenotic M1 might have suffered damage to the arteries through excess inflation of the balloon and stent. Indeed, in previous studies with coronary intervention, it has shown that remodeling pattern of coronary artery has relationship with the incidence of adverse cardiac events including post-interventional dissection.[39,42] Evaluation of wall morphology with high-resolution MRI may provide information about the optimum stent size and inflation pressure, and the present study suggests that preoperative investigation of the *RNF213* c.14576G>A may also improve the effectiveness of intracranial artery stenting.

The present study has some limitations. Only the outer diameter was measured on MRI as the morphological feature of ICAS and wall structure itself was not investigated. Wall imaging could observe more detailed influence of the *RNF213* c.14576G>A on the morphological characteristics of ICAS. In addition, to evaluate the effect of *RNF213* c.14576G>A on the normal intracranial artery, character-matched groups classified by the presence of *RNF213* c.14576G>A of healthy individuals, not only of atherosclerotic patients, must be compared.

CONCLUSION

This study indicates that *RNF213* c.14576G>A is associated with negative remodeling of ICAS.

Identification of the *RNF213* c.14576G>A may lead to optimum treatment of ICAS.

Financial support and sponsorship

This work was supported by a Grant-in-Aid for Scientific Research (B) (No. 25293304) to Dr. Saito; and a Grant-in-Aid for Young Scientists (B) (No. 15K19949) from the Japan Society for the Promotion of Science and grants from Mitsui Life Social Welfare Foundation, Tokyo, Japan to Dr. Miyawaki.

Conflicts of interest

There are no conflicts of interest.

REFERENCES

1. Ahn SH, Lee J, Kim YJ, Kwon SU, Lee D, Jung SC, *et al*. Isolated MCA disease in patients without significant atherosclerotic risk factors: A high-resolution magnetic resonance imaging study. Stroke 2015;46:697-703.
2. Arenillas JF. Intracranial atherosclerosis: Current concepts. Stroke 2011;42:S20-3.
3. Bruno R, Barzacchi M, Cartoni G, Antonelli M, Taddei S, Ghiadoni L. 4d. 06: Progression of carotid artery remodeling and stiffness in hypertensive patients: A prospective cohort study. J Hypertens 2015;33(Suppl 1):e62.
4. Burke AP, Kolodgie FD, Farb A, Weber D, Virmani R. Morphological predictors of arterial remodeling in coronary atherosclerosis. Circulation 2002;105:297-303.
5. Chen XY, Wong KS, Lam WW, Zhao HL, Ng HK. Middle cerebral artery atherosclerosis: Histological comparison between plaques associated with and not associated with infarct in a postmortem study. Cerebrovasc Dis 2008;25:74-80.
6. Chimowitz MI, Lynn MJ, Derdeyn CP, Turan TN, Fiorella D, Lane BF, *et al*. Stenting versus aggressive medical therapy for intracranial arterial stenosis. N Engl J Med 2011;365:993-1003.
7. Choi YJ, Jung SC, Lee DH. Vessel Wall Imaging of the Intracranial and Cervical Carotid Arteries. J Stroke 2015;17:238-55.
8. Chung GH, Kwak HS, Hwang SB, Jin GY. High resolution MR imaging in patients with symptomatic middle cerebral artery stenosis. Eur J Radiol 2012;81:4069-74.
9. Harteveld AA, Denswil NP, Siero JC, Zwanenburg JJ, Vink A, Pouran B, *et al*. Quantitative Intracranial Atherosclerotic Plaque Characterization at 7T MRI: An *Ex Vivo* Study with Histologic Validation. AJNR Am J Neuroradiol 2016;37:802-10.
10. Hitomi T, Habu T, Kobayashi H, Okuda H, Harada KH, Osafune K, *et al*. Downregulation of Securin by the variant RNF213 R4810K (rs112735431, G>A) reduces angiogenic activity of induced pluripotent stem cell-derived vascular endothelial cells from moyamoya patients. Biochem Biophys Res Commun 2013;438:13-9.
11. Jiang WJ, Cheng-Ching E, Abou-Chebl A, Zaidat OO, Jovin TG, Kalia J, *et al*. Multicenter analysis of stenting in symptomatic intracranial atherosclerosis. Neurosurgery 2012;70:25-30.
12. Jiang Y, Zhu C, Peng W, Degnan AJ, Chen L, Wang X, *et al*. Ex-vivo imaging and plaque type classification of intracranial atherosclerotic plaque using high resolution MRI. Atherosclerosis 2016;249:10-6.
13. Kaku Y, Morioka M, Ohmori Y, Kawano T, Kai Y, Fukuoka H, *et al*. Outer-diameter narrowing of the internal carotid and middle cerebral arteries in moyamoya disease detected on 3D constructive interference in steady-state MR image: Is arterial constrictive remodeling a major pathogenesis? Acta Neurochir 2012;154:2151-7.
14. Kamada F, Aoki Y, Narisawa A, Abe Y, Komatsuzaki S, Kikuchi A, *et al*. A genome-wide association study identifies RNF213 as the first Moyamoya disease gene. J Hum Genet. 2011;56:34-40.
15. Kanoke A, Fujimura M, Niizuma K, Ito A, Sakata H, Sato-Maeda M, *et al*. Temporal profile of the vascular anatomy evaluated by 9.4-tesla magnetic resonance angiography and histological analysis in mice with the R4859K mutation of RNF213, the susceptibility gene for moyamoya disease. Brain Res 2015;1624:497-505.
16. Kobayashi H, Matsuda Y, Hitomi T, Okuda H, Shioi H, Matsuda T, *et al*. Biochemical and Functional Characterization of RNF213 (Mysterin) R4810K, a Susceptibility Mutation of Moyamoya Disease, in Angiogenesis *In Vitro* and In Vivo. J Am Heart Assoc 2015;4:e002146.
17. Koo J. The Latest Information on Intracranial Atherosclerosis: Diagnosis and Treatment. Interv Neurol 2015;4:48-50.
18. Kume T, Okura H, Kawamoto T, Akasaka T, Toyota E, Watanabe N, *et al*. Relationship between coronary remodeling and plaque characterization in patients without clinical evidence of coronary artery disease. Atherosclerosis 2008;197:799-805.
19. Kuroda S, Kashiwazaki D, Akioka N, Koh M, Hori E, Nishikata M, *et al*. Specific Shrinkage of Carotid Forks in Moyamoya Disease: A Novel Key Finding for Diagnosis. Neurol Med Chir (Tokyo) 2015;55:796-804.
20. Kurosaki Y, Yoshida K, Fukumitsu R, Sadamasa N, Handa A, Chin M, *et al*. Carotid artery plaque assessment using quantitative expansive remodeling evaluation and MRI plaque signal intensity. J Neurosurg 2016;124:736-42.
21. Liu W, Morito D, Takashima S, Mineharu Y, Kobayashi H, Hitomi T, *et al*. Identification of RNF213 as a susceptibility gene for moyamoya disease and its possible role in vascular development. PLoS One 2011;6:e22542.
22. Miyatake S, Miyake N, Touho H, Nishimura-Tadaki A, Kondo Y, Okada I, *et al*. Homozygous c.14576G>A variant of RNF213 predicts early-onset and severe form of moyamoya disease. Neurology 2012;78:803-10.
23. Miyawaki S, Imai H, Shimizu M, Yagi S, Ono H, Mukasa A, *et al*. Genetic variant RNF213 c.14576G>A in various phenotypes of intracranial major artery stenosis/occlusion. Stroke 2013;44:2894-7.
24. Miyawaki S, Imai H, Takayanagi S, Mukasa A, Nakatomi H, Saito N. Identification of a genetic variant common to moyamoya disease and intracranial major artery stenosis/occlusion. Stroke 2012;43:3371-4.
25. Pasterkamp G, Hillen B, Borst C. Arterial remodelling by atherosclerosis. Semin Interv Cardiol 1997;2:147-52.
26. Pasterkamp G, Wensing PJ, Post MJ, Hillen B, Mali WP, Borst C. Paradoxical arterial wall shrinkage may contribute to luminal narrowing of human atherosclerotic femoral arteries. Circulation 1995;91:1444-9.
27. Prati F, Mallus MT, Parma A, Lioy E, Pagano A, Boccanelli A. Incidence of compensatory enlargement and paradoxical shrinkage of coronary arteries in presence of atherosclerotic lesions: An intracoronary ultrasound study based on multiple cross-section analysis per artery. G Ital Cardiol 1998;28:1063-71.
28. Qiao Y, Anwar Z, Intrapiromkul J, Liu L, Zeiler SR, Leigh R, *et al*. Patterns and Implications of Intracranial Arterial Remodeling in Stroke Patients. Stroke 2016;47:434-40.
29. Ryoo S, Cha J, Kim SJ, Choi JW, Ki CS, Kim KH, *et al*. High-resolution magnetic resonance wall imaging findings of Moyamoya disease. Stroke 2014;45:2457-60.
30. Ryoo S, Lee MJ, Cha J, Jeon P, Bang OY. Differential Vascular Pathophysiologic Types of Intracranial Atherosclerotic Stroke: A High-Resolution Wall Magnetic Resonance Imaging Study. Stroke 2015;46:2815-21.
31. Saam T, Habs M, Buchholz M, Schindler A, Bayer-Karpinska A, Cyran CC, *et al*. Expansive arterial remodeling of the carotid arteries and its effect on atherosclerotic plaque composition and vulnerability: An in-vivo black-blood 3T CMR study in symptomatic stroke patients. J Cardiovasc Magn Reson 2016;18:11.
32. Schoenhagen P, Ziada KM, Vince DG, Nissen SE, Tuzcu EM. Arterial remodeling and coronary artery disease: The concept of "dilated" versus "obstructive" coronary atherosclerosis. J Am Col Cardiol 2001;38:297-306.
33. Scholz B, Korn C, Wojtarowicz J, Mogler C, Augustin I, Boutros M, *et al*. Endothelial RSPO3 Controls Vascular Stability and Pruning through Non-canonical WNT/Ca (2+)/NFAT Signaling. Dev Cell 2016;36:79-93.
34. Smits PC, Bos L, Quarles van Ufford MA, Eefting FD, Pasterkamp G, Borst C. Shrinkage of human coronary arteries is an important determinant of de novo atherosclerotic luminal stenosis: An *in vivo* intravascular ultrasound study. Heart. 1998;79:143-7.
35. Sonobe S, Fujimura M, Niizuma K, Nishijima Y, Ito A, Shimizu H, *et al*. Temporal profile of the vascular anatomy evaluated by 9.4-T magnetic resonance angiography and histopathological analysis in mice lacking RNF213: A susceptibility gene for moyamoya disease. Brain Res. 2014;1552:64-71.
36. Suri MF, Qiao Y, Ma X, Guallar E, Zhou J, Zhang Y, *et al*. Prevalence of Intracranial Atherosclerotic Stenosis Using High-Resolution Magnetic Resonance Angiography in the General Population: The Atherosclerosis

Risk in Communities Study. Stroke 2016;47:1187-93.
37. Uchiyama S, Sakai N, Toi S, Ezura M, Okada Y, Takagi M, *et al*. Final Results of Cilostazol-Aspirin Therapy against Recurrent Stroke with Intracranial Artery Stenosis (CATHARSIS). Cerebrovasc Dis Extra 2015;5:1-13.
38. Varnava AM, Mills PG, Davies MJ. Relationship between coronary artery remodeling and plaque vulnerability. Circulation 2002;105:939-43.
39. Wexberg P, Gyongyosi M, Sperker W, Kiss K, Yang P, Hassan A, *et al*. Pre-existing arterial remodeling is associated with in-hospital and late adverse cardiac events after coronary interventions in patients with stable angina pectoris. J Am Col Cardiol 2000;36:1860-9.
40. Xu P, Lv L, Li S, Ge H, Rong Y, Hu C, *et al*. Use of high-resolution 3.0-T magnetic resonance imaging to characterize atherosclerotic plaques in patients with cerebral infarction. Exp Ther Med 2015;10:2424-8.
41. Xu WH, Li ML, Gao S, Ni J, Zhou LX, Yao M, *et al*. *In vivo* high-resolution MR imaging of symptomatic and asymptomatic middle cerebral artery atherosclerotic stenosis. Atherosclerosis 2010;212:507-11.
42. Yamagishi M, Terashima M, Awano K, Kijima M, Nakatani S, Daikoku S, *et al*. Morphology of vulnerable coronary plaque: Insights from follow-up of patients examined by intravascular ultrasound before an acute coronary syndrome. J Am Coll Cardiol 2000;35:106-11.
43. Yang WJ, Chen XY, Zhao HL, Niu CB, Xu Y, Wong KS, *et al*. *In vitro* Assessment of Histology Verified Intracranial Atherosclerotic Disease by 1.5T Magnetic Resonance Imaging: Concentric or Eccentric? Stroke 2016;47:527-30.
44. Zhao DL, Deng G, Xie B, Ju S, Yang M, Chen XH, *et al*. High-resolution MRI of the vessel wall in patients with symptomatic atherosclerotic stenosis of the middle cerebral artery. J Clin Neurosci 2015;22:700-4.
45. Zhu XJ, Du B, Lou X, Hui FK, Ma L, Zheng BW, *et al*. Morphologic characteristics of atherosclerotic middle cerebral arteries on 3T high-resolution MRI. AJNR Am J Neuroradiol 2013;34:1717-22.
46. Zhu X, Liu L, He X, Zhang X, Hu L, Du B, *et al*. Wall thickening pattern in atherosclerotic basilar artery stenosis. Neurol Sci 2016;37:269-76.